Tellus (1982), *34*, 481–489

Bubble entrainment in breaking wind waves

By MOMOKI KOGA,[1] *Physical Oceanography Laboratory, Geophysical Institute, Tohoku University, Sendai 980, Japan*

(Manuscript received March 13; in final form December 21, 1981)

ABSTRACT

Processes of bubble formation and spreading in breaking wind waves are experimentally investigated in a wind-wave tank. The distribution and movement of bubbles relative to the wave form are measured using photographic techniques. The main mechanism of bubble formation in these waves is intermittent bubble entrainment by an ordered convergent flow on the leading slope near the crest. This conclusion is supported by a simple experiment for modeling the bubble entrainment, where a small jet of water is injected into water whose surface is at rest: bubbles are entrained by the water jet. In the oceans, the mechanism under consideration will be important in understanding the breaking process of smaller scale waves superposed on dominant waves. A model experiment also shows that the existence of a stagnation point on a water surface (convergent flow) is not a sufficient condition for bubble entrainment. The downward force of the convergent flow must be greater than the restoring force of the surface tension at the stagnation point for bubble entrainment to occur.

1. Introduction

Bubbles and foam have much influence on gas exchange through the sea surface, and also on the reflection and scattering of light, microwaves and sound waves. The bursting of bubbles on the sea surface produces many sea water droplets. Measurements in the ocean under moderate wind conditions have shown that most bubbles near the surface are caused by wave breaking (Kolovayev, 1976; Medwin, 1977; Johnson and Cooke, 1979), though small bubbles may be produced by other mechanisms such as biological and chemical changes in the solubility of air (Blanchard and Woodcock, 1957; Medwin, 1977). Toba (1961) and Glotov et al. (1962) have also measured the distribution of bubbles in laboratory experiments. However, they measured only the mean vertical distribution of the bubble concentration and the size distribution. Toba et al. (1975) analyzed the movement of entrained bubbles with respect to the phase of the waves and reported intermittent bubble entrainment caused by the convergence of the surface current at the downwind slope near the crest. However, we do not as yet have enough information regarding the distribution and movement of bubbles, which would clarify the mechanisms of bubble formation and spreading.

The aim of the present study is to fill this gap. Based on experimental results, a mechanism of bubble formation and spreading in relation to wind-wave breaking is proposed.

2. Measurements of formation and distribution of bubbles

The formation of bubbles by breaking wind waves and the process of bubble spreading were studied by making photographic measurements in a wind-wave tank 20 m long, 0.6 m wide and 1.2 m high containing fresh water 0.6 m in depth. The reference wind speed, U_r, measured at the center of the inlet section of the wind-wave tank was 16 m s^{-1} and the fetch, F, was 16 m. Under these conditions, the significant wave height and period were 9.0 cm and 0.73 s, respectively. The measurements were made with two photographic systems. In the first system a side view of wind waves was taken. In the second system ("view from below"),

[1] Present address: Physical Oceanography Laboratory, Department of Geophysics, Hokkaido University, Sapporo 060, Japan.

 0040-2826/82/050481-09$02.50/0

the wave surfaces were photographed from the side of the tank but with a mirror placed at the bottom of the tank. The view from below clearly shows the micro-configurations of the wave surface and the horizontal distribution of bubbles, which can not be clearly seen in side-view pictures. In each system, a 35 mm still camera faces a light source—a strobe which causes shadow images of bubbles and micro-configurations of the wave surface (shadowgraph photographic technique). Details of this technique have already been described by Koga (1981).

Examples of the side view of breaking wind waves are shown in Fig. 1. Fig. 1a shows that bubbles distribute along a line which starts from the leading slope near the crest. Lines of bubbles are also seen in Fig. 1b. They extend from the crest area to the windward slope of the wave. In Fig. 1c, scattered patterns of lines of bubbles are seen from the windward slope to the trough. These lines of bubbles can be seen in almost all side-view photographs, when bubble clusters and large bubbles occur.

These photographs show the process of bubble formation and spreading. Most bubbles are initially transported fairly deep down under the leading slope of the wave by an intermittent entrainment caused by an ordered downward water flow starting somewhere on the leading slope near the crest. As the wave progresses, bubbles shift backwards relative to the wave form. Meanwhile, the line pattern of bubbles is disturbed by turbulence and by the fact that rising bubbles have different velocities.

Fig. 2 shows the mean pattern of bubble distribution along a representative wave. In the present case, bubble clusters (hatched and cross-hatched areas) are concentrated mostly between the crest and the leading slope, and they are found down to a depth of about half the wave height. Separated bubbles (diameter $\geqslant 0.85$ mm) are mainly found between the crest and the windward slope, and the number density sharply decreases with depth at a depth of about one wave height. The line of sharp decrease of the number density is nearly parallel to the windward slope of the water surface and shows the mean lower limit to which the lines of bubbles can penetrate.

The movement of the bubbles was measured by use of a multi-colored overlapping exposure photographic technique (MOET) described by Koga (1981). We can estimate the water velocity distribution arising from the movement of the bubbles by subtracting the terminal velocity of rising bubbles in still water from the measured bubble velocity. As terminal velocities we used values measured by Datta et al. (1950). Fig. 3 shows an example of the velocity distribution of water flow relative to the wave form. The slantingly downward flow, probably intermittent, is seen at the tip (the lowest point) of the bubble cluster under the leading slope near the crest; the water particles under the windward slope move nearly parallel to the slope.

Calculations of the average speed and direction of the downward flow were based on the movement of bubble clusters beneath the water surface at the leading slope, using 44 photographs with bubble entrainments. The results are shown in Fig. 4. This figure shows that the flow speed ranges from about 0.4 m s^{-1} to 1.2 m s^{-1} with a mean value of about 0.8 m s^{-1}. The direction varies from 190° to 230° with a mean value of 215° (35° downward from the horizontal). The presence of such a strong downward flow in wind waves with bubble formations was also reported by Toba et al. (1975).

The existence of the downward flow is also verified by a view of the wave surface from below. Fig. 5a shows fine configurations of a bubble-entraining wave surface viewed from below. A clear line which separates the region with and without bubbles is seen in the middle of the photograph. In the upwind area from this line, many irregular ripples and entrained bubbles can be seen. In the downwind area, the wave surface is much smoother. Along this line the surface water converges and it is the downward flow that causes the bubble entrainment. On the other hand, in cases without bubble entrainment (Fig. 5b), there is no clear line on the wave surface and irregular ripples are seen in the entire area of the photograph. Though these photographs were taken with fixed conditions of wind and fetch and show the same area of the leading slope, the surface configurations are quite different.

Our photographic measurements indicate that the main mechanism of bubble formation in breaking short wind waves in a wind-wave tank is intermittent bubble entrainment caused by an ordered, convergent flow on the leading slope near the crest. This supports the previous observations made by Toba et al. (1975) and gives a clearer picture of bubble entrainment. The entrained

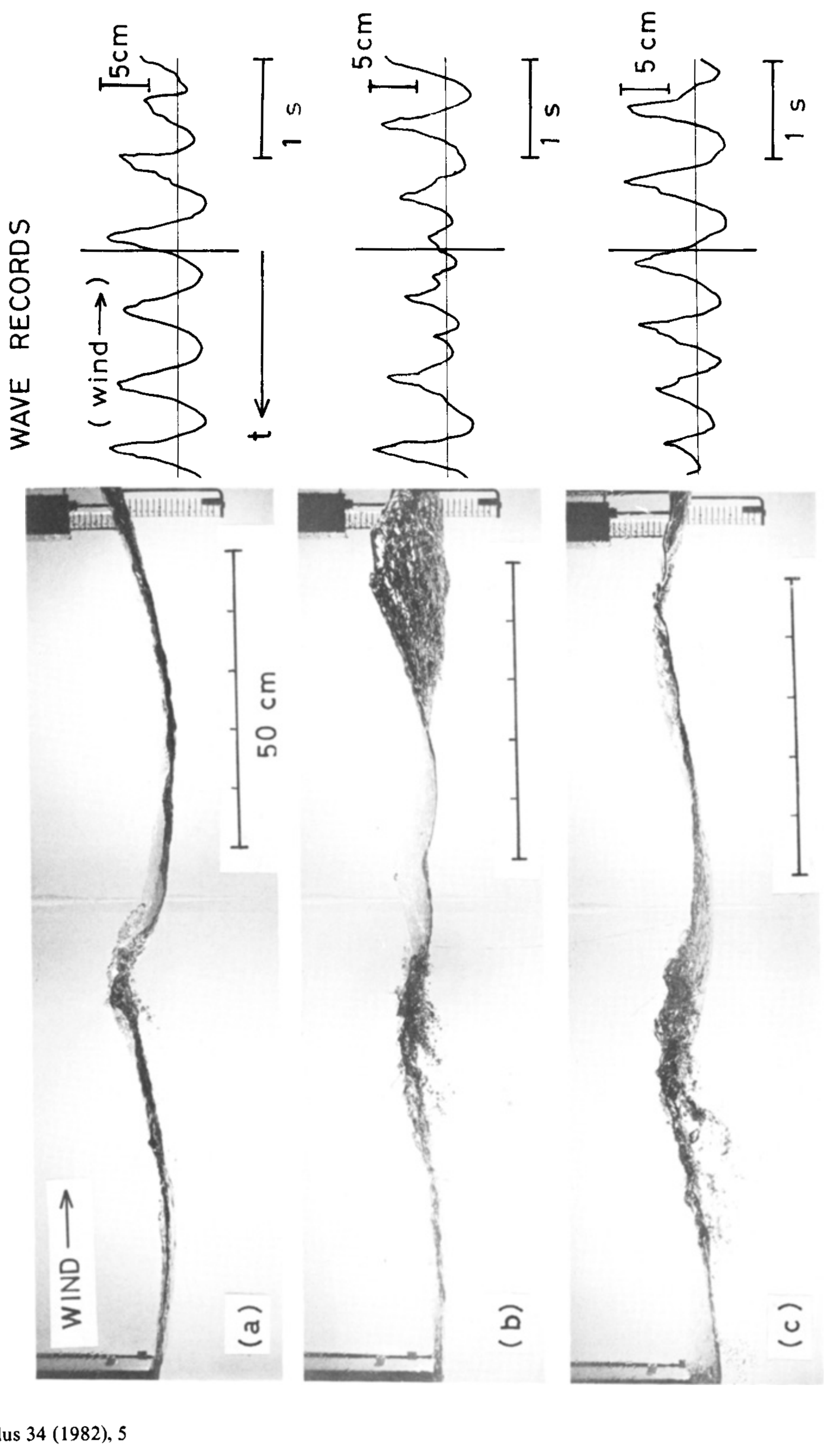

Fig. 1. Breaking wind waves for the case of $F = 16$ m and $U_r = 16$ m s^{-1}. Wave records were taken at $F = 16.4$ m by a wave gauge which is seen on the right of each photograph, together with a scale. The time when the photos were taken is marked by a vertical line on the wave records.

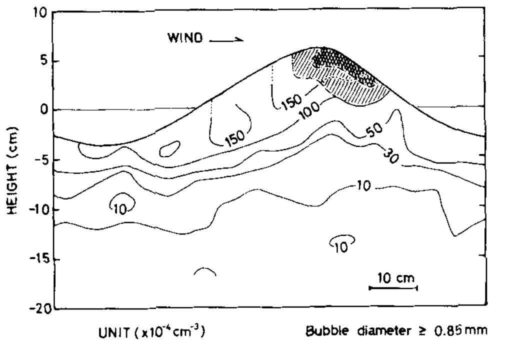

Fig. 2. Mean distribution of bubbles along a representative wave. The figure was drawn using 48 side-view photographs. Each of the photographs has a width of about ¼ of that of the photographs in Fig. 1. The hatched and cross-hatched areas indicate the bubble cluster appearance, with a probability of 10% and 20%, respectively. The contour lines indicate the number density distribution of bubbles.

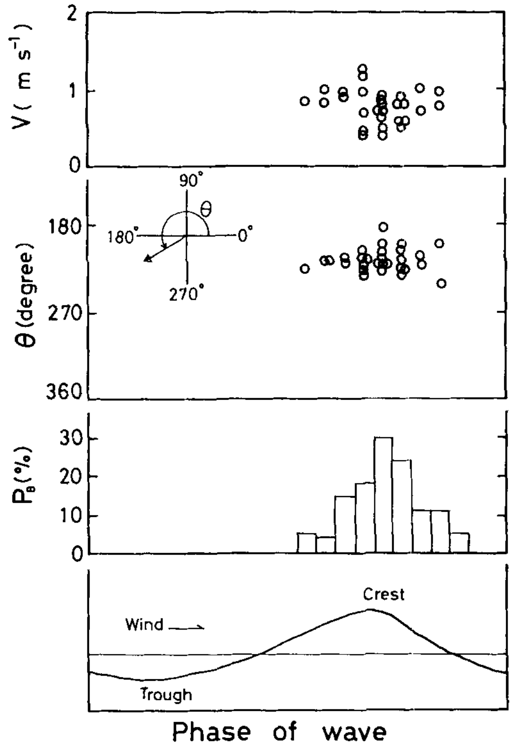

Fig. 4. Distribution of the speed, v, and direction, θ, of the downward flow under the leading slope of the breaking waves. Distribution of the bubble clusters beneath the wave surface is also shown by P_B, which is the probability of their presence.

bubbles can be transported fairly deeply by the ordered convergent flow itself, and are distributed along a line. It should be noted that some bubbles may be entrained at sharpened troughs of Crapper-type wavelets superposed on the wind-wave crest as suggested by Toba (1961). However, bubbles created by this entrainment mechanism are only diffused by turbulence and do not form distinctive lines.

3. A simple model experiment for bubble entrainment

When the surface current constantly exceeds the phase speed of the wave near the crest, a stagnation point exists on the leading slope and convergence occurs at the stagnation point as explained in Fig. 6a. A simple model of bubble entrainment caused by convergent flow is introduced. A small jet of

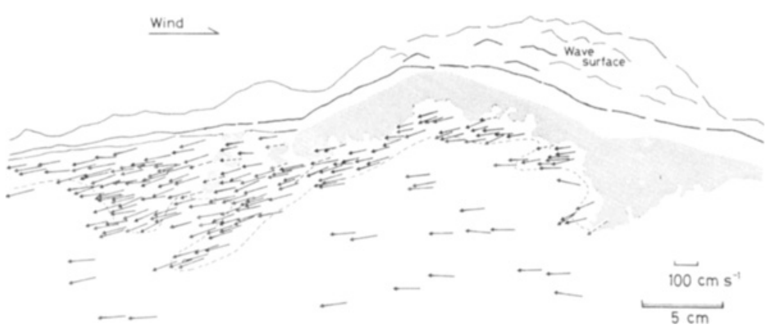

Fig. 3. An example of the velocity field of water flow relative to the wave form. Solid arrows and broken arrows indicate the velocity of the water flow estimated from the movement of isolated bubbles and from that of bubble clusters, respectively. In the shaded area bubble clusters appeared. The area between the dashed line and the edge of the shaded area is the region where many isolated bubbles are seen.

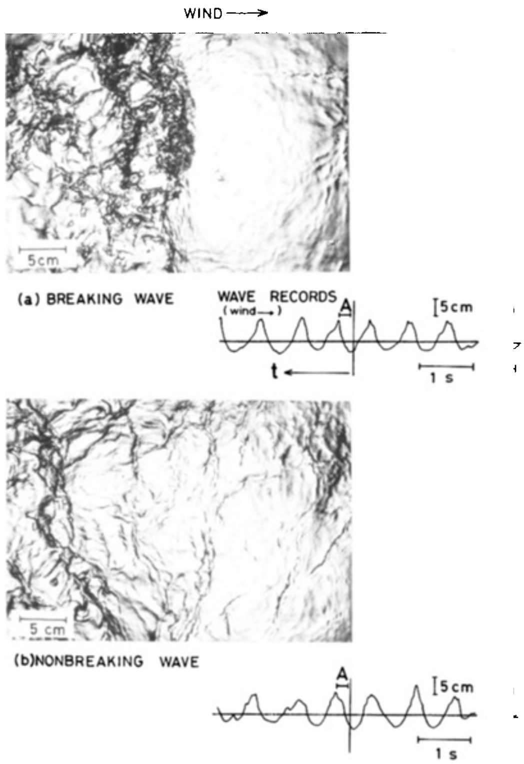

Fig. 5. View of the wave surface from below with and without bubble entrainment. The time when the photos were taken is marked with a vertical line in the wave record shown beneath each photograph. The horizontal line marked A represents the extent of the photographed wave surface.

water was injected into water whose surface was at rest, causing bubble entrainment. Fig. 6b shows a schematic picture of the model. The side having an obtuse angle (angle greater than 90°) between the injected jet and the water at rest can be a simple model for bubble entrainment in breaking wind waves.

The experimental procedure was as follows. The water from an overflow tank was injected into water whose surface was at rest through a nozzle which regulated the water flow to form the water jet. The velocity of the injected water jet was controlled by changing the vertical distance between the water surface at rest and the over-flow tank. The distance between the outlet of the nozzle and the water surface at rest was about 1 cm. The shapes and sizes of the nozzle used are listed in Table 1. The nozzle with a rectangular cross section (H) was selected to create a two-dimensional jet flow. Nozzles having circular cross sections with various curvatures (A, C and E) were also used for investigating the effect of jet-flow curvature on bubble entrainment. A tank (8 m long, 0.15 m wide, 0.47 m deep) was used as a container for still, fresh water, into which the water jet was injected. The size of the tank was large enough to avoid disturbance effects from the side walls and the bottom.

Examples of bubble entrainment are shown in Fig. 7 for various inclinations ranging from 15° to

Table 1. *Nozzles with various curvatures used for the model experiment*

Nozzle	Shape of the nozzle mouth	Mouth size, diameter ϕ (cm)	Curvature $K \equiv 2/\phi$ (cm^{-1})
H	rectangle (2.00 cm × 0.12 cm)	—	0
A	circle	0.46	4.35
C	circle	0.31	6.45
E	circle	0.16	12.5

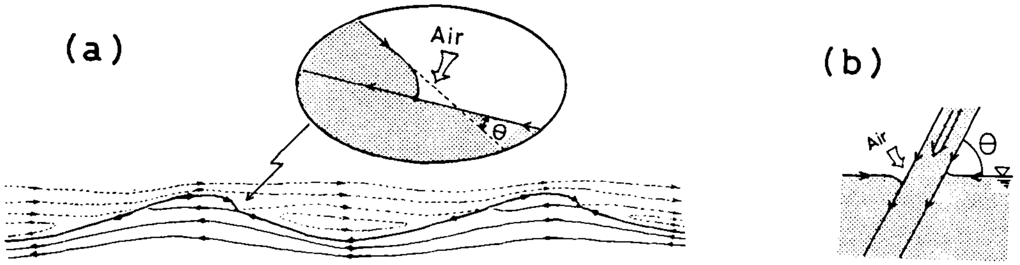

Fig. 6. A model of bubble entrainment. (a) Schematic flow pattern of air and water for constantly breaking wind waves in a coordinate moving with the wave. (b) Injection of a small jet of water into water whose surface is at rest.

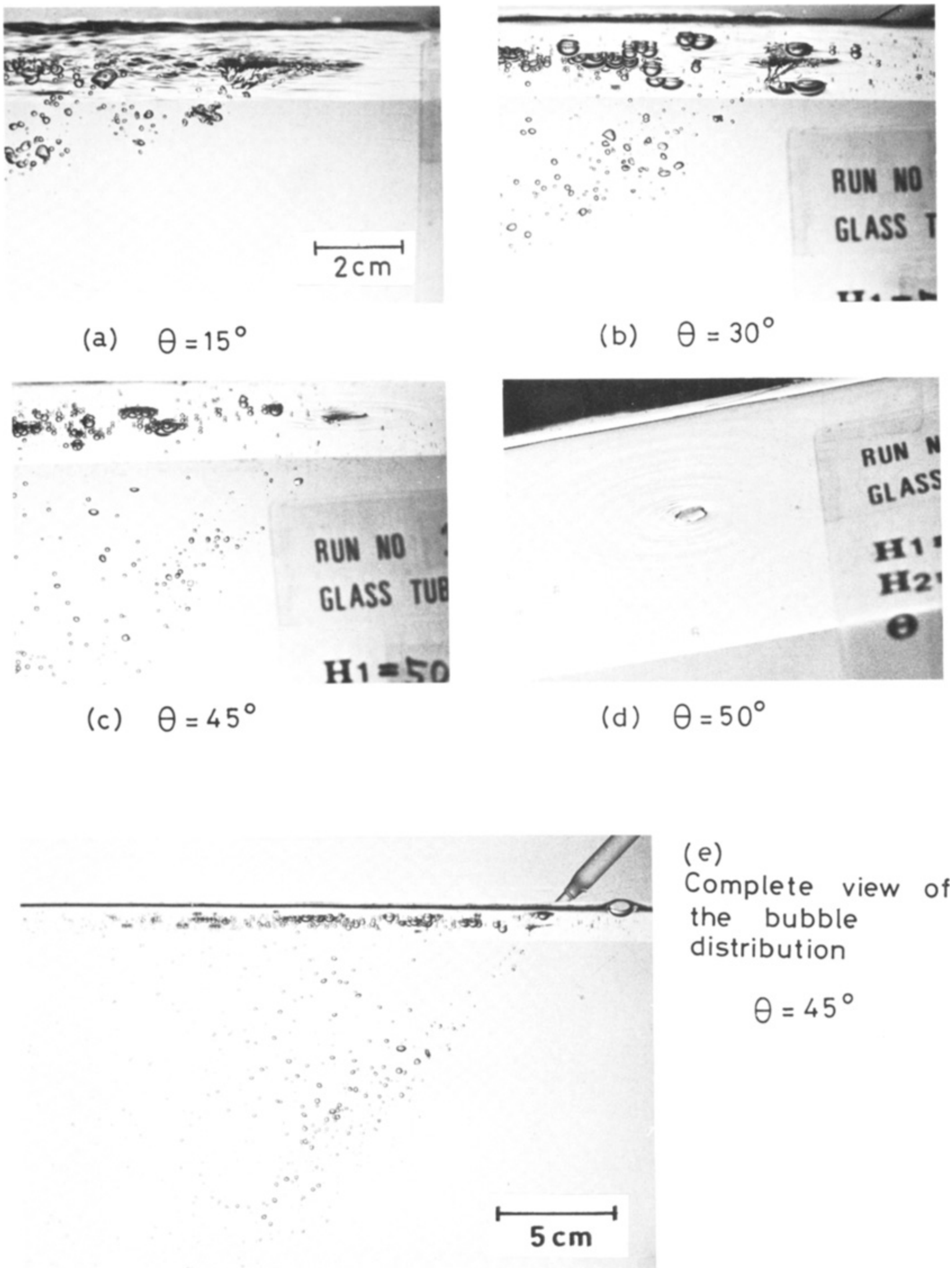

Fig. 7. Examples of bubble entrainment caused by injected flow through nozzle A, for various inclinations ranging from 15° to 50°. $v = 2.12$ m s^{-1}.

50° (nozzle A, $v = 2.12$ m s^{-1}). In Figs. 7a,b,c, bubbles are entrained at the tip of the wedge-shaped cavity on the water surface, which is formed by the convergence of surface flow around the injection. For the smaller injection angle θ, the wedge-shaped cavity is large and unstable, and larger bubbles are entrained. With increasing θ, the cavity and the bubbles become smaller. Especially in the case of small injection velocity, bubbles are not entrained at all for angles larger than the critical angle of injection, θ_c. θ_c varies with nozzle type and injection velocity. In Fig. 7d, which nearly corresponds to the critical condition, the conspicuous cavity is not seen and few bubbles are entrained.

The configurations of the water surface around the jet are schematically shown in Fig. 8, which shows a radial cross section for the case of a circular water jet. In the case of bubble entrainment (with moderate injection velocity), the cavity and bubbles are seen on the side of the injection having an obtuse angle. But on the side having an acute angle, neither cavity nor bubble entrainment is seen, apart from in the case of high injection velocity (Fig. 8a). In cases without bubble entrainment (with low injection velocity), the cavity is not seen even on the obtuse angle side of the injection, and the water surface around the jet is rather smooth (Fig. 8b).

A complete view of the bubble distribution is shown in Fig. 7e. The entrained bubbles can be transported fairly deeply by the injected jet flow. This supports the previous conclusion that the lines of bubbles in breaking wind waves are caused by intermittent bubble entrainment due to an ordered convergent downward flow on the leading slope near the crest. The diameter, d, of the entrained bubbles ranged approximately from 25 μm to 4500 μm. Bubble sizes larger than 500 μm were measured photographically. Bubbles smaller than 500 μm were collected with a small box and their sizes were measured with a microscope. Glotov et al. (1962) found the lower limit of bubble diameter to be about 50 μm for bubbles formed by wind waves breaking in a wind-wave tank. Therefore, the lower limit of bubble diameter in the model experiment is approximately the same as that in breaking wind waves.

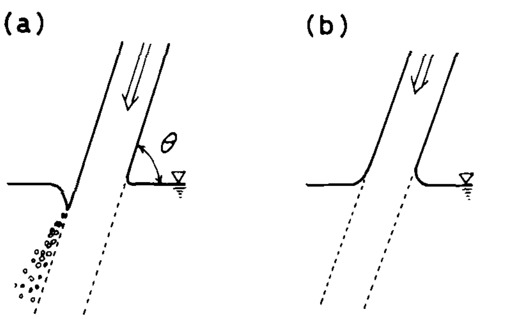

Fig. 8. Schematic representation of the configurations of the water surface around the jet flow. (a) Configuration in the case of an occurrence of bubble entrainment (moderate velocity of injection). (b) Configuration in the case of an absence of bubble entrainment (low velocity of injection).

The critical condition for the occurrence of bubble entrainment is shown in Fig. 9a, where the critical angle θ_c is related to the injection velocity v and the nozzle type (curvature K). θ_c increases with increasing values of v and decreases with increasing values of K. This indicates that bubble entrainment takes place when the downward force due to the injection flow is greater than the restoring force due to surface tension.

It should be mentioned here that the critical angle, θ_c, could not be measured when v was small, since the water jet for small θ had a tendency to bend downward. Especially for the rectangular cross section jet (H nozzle), θ_c could not be measured with sufficient accuracy, since the cross section of the jet flow had a tendency to become round soon after leaving the mouth of the nozzle. Also, θ_c could not be measured when v was large, because the bubble entrainment process became highly unstable.

At the critical point for bubble entrainment, the downward force of the jet flow and the restoring upward pressure force of surface tension are balanced. The downward force is assumed to be proportional to the dynamic pressure $\frac{1}{2}\rho v^2$ of the jet flow, and the upward pressure can be written as $T(1/r_1 + 1/r_2)$, where ρ is the density of water, v the velocity of the jet flow, T the surface tension, and r_1 and r_2 are the radii of curvature of the water surface in the vertical and the horizontal sections, respectively (i.e. $1/r_2 \approx K$). The ratio W_e between the two pressures is given by

$$W_e = \frac{1}{2}\rho v^2 \Big/ T\left(\frac{1}{r_1} + \frac{1}{r_2}\right) = (\rho r_1 v^2/2T)/(1 + r_1/r_2). \quad (1)$$

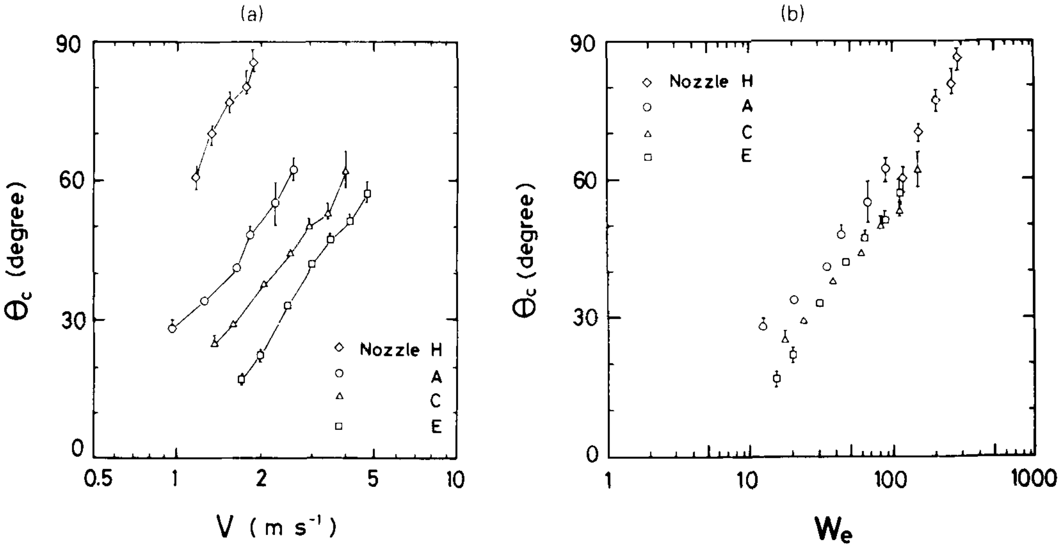

Fig. 9. Critical condition for bubble entrainment. (a) Relation between the critical angle, θ_c, and the injection velocity, v, for various curvatures of the injected jet flow (nozzles H, A, C and E). (b) Relation between θ_c and the non-dimensional parameter W_e.

This non-dimensional parameter W_e is some kind of a Weber number. Using the parameter W_e, we can modulate Fig. 9a to get Fig. 9b. We assume that r_1 has the same value for all the different nozzles used. r_1 is obtained on the condition that values of θ_c are plotted best as a unique function of W_e. r_1 is 1.25 cm in the present experiment.

The present results may be insufficient for clarifying the critical condition of bubble entrainment in breaking wind waves. However, they have shown the following facts. The presence of the downward convergent flow around a stagnation point at the water surface does not necessarily mean the occurrence of bubble entrainment in the convergent area. The critical condition is clearly controlled by the velocity v, the angle θ and the curvature K of the injection jet flow, and is closely related to the non-dimensional number W_e. The ordered downward flow can then transport the entrained bubbles fairly deeply.

4. Discussion

Our two experiments show that the main mechanism of bubble formation in breaking short wind waves in a wind-wave tank is intermittent bubble entrainment by an ordered downward flow at the leading slope near the crest. The present mechanism is much different from that usually proposed for spilling-type breaking waves (e.g. Cokelet, 1977), in which bubbles are assumed to be formed by a turbulent mixing of spilling water with air. The spreading process of bubbles in the model under consideration is also different from that of spilling-type breaking waves. In spilling-type breaking waves, clusters of bubbles can only be diffused by the turbulence near the water surface, as assumed in the model of Longuet-Higgins and Turner (1974). On the other hand, in the case of bubble entrainment by an ordered downward flow, bubbles are easily transported downward by the flow itself as is seen from the lines of bubbles in Fig. 1.

Our wind-wave tank experiment was conducted with fairly high wind for realizing wind-wave breaking at a short fetch of 20 m. In this case, the ratio of the phase speed to the mean surface drift, c/q_0, is about 1, which is smaller than that usually found in the ocean. According to Phillips (1977), the surface drift is unimportant for the breaking of wind waves, if $c/q_0 \gg 1$. If this is right and if we consider the difference in values of c/q_0 between the case of the laboratory and that of the ocean, the present mechanism of bubble formation may be of secondary importance in the breaking process of dominant larger waves in the oceans. However, it is important at least in the breaking process of many smaller waves superposed on the dominant waves, since the surface drift is often comparable to the phase speed of these smaller waves. Therefore, the mechanism under consideration is important in gas exchange between air and sea and in the downward transportation of various matter on and near the sea surface.

Furthermore, we can examine the criterion for wind-wave breaking on the basis of the present experimental results. As clarified by the model experiment in Section 3, the existence of stagnation points or convergent flows is not a sufficient condition for bubble entrainment. As for the essential condition of droplet production, a similar fact has been reported by Koga (1981). If wind-wave breaking is defined by the occurrence of bubble entrainment and droplet production, then it is not equivalent to the appearance of stagnation points. That the conditions for the occurrence of bubble entrainment or droplet production and for the appearance of stagnation points are not identical, was also considered by Banner and Phillips (1974) in their discussion of the incipient breaking mechanism, though they did not refer to the mechanisms of bubble entrainment and droplet production.

For the following reasons, it is expected that the critical velocity for bubble entrainment is less than 0.5 m s^{-1}. The value of θ in breaking wind waves will be generally less than 30°; if the convergence of surface water takes place two-dimensionally, the non-dimensional parameter W_e is expected to be less than 20 (Fig. 9b). Using eq. (1), this gives a value of 0.5 m s^{-1} for v. This value of 0.5 m s^{-1} will not greatly contradict our measurement of the downward velocity in breaking wind waves (Fig. 4), in which the velocity ranged from about 0.4 m s^{-1} to 1.2 m s^{-1}. However, the actual condition for bubble entrainment may be further controlled and modulated by the horizontal extent of the downward flow, and the flow unsteadiness.

5. Acknowledgments

The author wishes to express his sincere thanks to Professor Y. Toba of Tohoku University for introducing him to this field of work and for his constant valuable advice and encouragement. Thanks are also due to Dr S. Kawai and Dr K. Okuda of Tohoku University for their valuable suggestions and encouragement and to Dr P. S. Joseph for his critical reading of the manuscript.

REFERENCES

Banner, M. L. and Phillips, O. M. 1974. On the incipient breaking of small scale waves. *J. Fluid Mech. 65*, 647–656.

Blanchard, D. C. and Woodcock, A. H. 1957. Bubble formation and modification in the sea and its meteorological significance. *Tellus 9*, 145–158.

Cokelet, E. D. 1977. Breaking waves. *Nature 267*, 769–774.

Datta, R. L., Napier, D. H. and Newitt, D. M. 1950. The properties and behaviour of gas bubbles formed at a circular orifice. *Trans. Instr. Chem. Engrs. 28*, 14–26.

Glotov, V. P., Kolovayev, P. A. and Neuimin, G. G. 1962. Investigation of the scattering of sound by bubbles generated by an artificial wind in sea water and the statistical distribution of bubble sizes. *Soviet physics—Acoustics 7*, 341–345.

Johnson, B. D. and Cooke, R. C. 1979. Bubble populations and spectra in coastal waters: a photographic approach. *J. Geophys. Res. 84*, 3761–3766.

Koga, M. 1981. Direct production of droplets from breaking wind waves—its observation by a multicolored overlapping exposure photographing technique. *Tellus 33*, 552–563.

Kolovayev, P. A. 1976. Investigation of the concentration and statistical size distribution of wind-produced bubbles in the near-surface ocean layer. *Oceanology, Engl. Transl. 15*, 659–661.

Longuet-Higgins, M. S. and Turner, J. S. 1974. An "entraining plume" model of a spilling breaker. *J. Fluid Mech. 63*, 1–20.

Medwin, H. 1977. *In situ* acoustic measurements of microbubbles at sea. *J. Geophys. Res. 82*, 971–976.

Phillips, O. M. 1977. *The dynamics of the upper ocean*, 2nd edition. Cambridge Univ. Press, p. 336.

Toba, Y. 1961. Drop production by bursting of air bubbles on the sea surface (III). Study by use of a wind flume. *Memoirs Coll. Sci. Univ. Kyoto, Ser. A, 29*, 313–344.

Toba, Y., Tokuda, M., Okuda, K. and Kawai, S. 1975. Forced convection accompanying wind waves. *J. Oceanogr. Soc. Japan 31*, 192–198.